Comparison between experiment and two simulation strategies for the extraction of focused ion beams

Orson Sutherland,[a] John Keller, Michael Irzyk, and Rod Boswell
Plasma Research Laboratory, RSPhysSE, Australian National University, 0200 Canberra, Australia

(Received 18 February 2003; accepted 16 March 2004; published online 21 June 2004)

Computer simulation codes for the extraction of ion beams have been used for over three decades. Here we describe medium current extraction (~1 mA) from a high density plasma source ($>10^{12}\,\mathrm{cm}^{-3}$) with a three electrode extraction system and compare the extracted current and the angular divergence with the results of two computer simulation programs. The first is called PBgun and is a commercially available ray tracing code; the second, called simulation d'extraction de faisceaux d'ions (SEFI) uses a particle-in-cell code to simulate the plasma and ion beam. It is the purpose of this article to ascertain whether these codes can adequately model the plasma/beam interface and hence successfully predict the extracted current and beam form across a broad range of extraction parameters. We found that SEFI could accurately predict the function of extracted current versus extraction voltage and that PBgun gave accurate simulations when the current or current density could be specified near the meniscus. Also for a thin plasma aperture and a fixed current at the meniscus, PBgun gave roughly 60% of the functional dependence of the extracted current on the extraction voltage and the other 40% on variations in the plasma pre-sheath. Both codes had some error from beam crossing near the axis which changed the amount of meniscus curvature predicted. [DOI: 10.1063/1.1753669]

I. INTRODUCTION

Ion beams have been used for decades for altering the properties of surfaces.[1] Often, the source of ions is an ionized gas, a plasma, from which the ions are extracted by an arrangement of electrodes. In the case of positive ions, the electrode contacting the plasma is set to a potential of some kilovolts positive, the ions being extracted by the electric field created to the last, earthed, electrode. Compared to liquid metal ion sources, which have enabled ion optics to approach electron optics in brightness[2,3] ($>10^6\,\mathrm{A\,cm^{-2}\,sr^{-1}}$), plasmas pose a number of problems which can lead to considerable beam degradation. Among these problems are: perpendicular acceleration of ions by strong radial space charge fields in the extracted beam, finite ion temperature both parallel and perpendicular to the axis of the beam, and the normal optical aberrations associated with the manipulation of charged particle beams.

In theory electrodes can be designed to be almost aberration free. In most practical situations, however, ideal electrode designs cannot be reproduced exactly due to limitations in materials and manufacturing techniques and so some level of aberration is to be expected. Typically, the design of practical electrodes is done by educated trial and error, and therefore, in an effort to reduce the lead time on prototyping, some form of modeling tool is generally employed. Many are available, such as PBgun,[4] IGUN,[5] and AXCEL-GSI[6] for two-dimensional (2D) simulation and KOBRAS[7] for three-dimensional (3D) simulation. In this article we compare a typical ray-tracing code, PBgun, to a particle-in-cell (PIC) code called simulation d'extraction de faisceaux d'ions (SEFI) and a single aperture, three electrode extraction experiment.

A major difficulty in the simulation of ion extraction from a plasma is the question of how to model the plasma and the plasma sheath at the extraction aperture. This plasma boundary is known as the plasma meniscus and its shape determines the form and distribution of the extracted beam. In a PIC, if the plasma is assumed to be collisionless (a good assumption under a wide range of experimental situations), no model other than the macroparticle, Poisson's equation, and Newton's second law is used to determine the state of particles at any point in the system; instead structures such as the meniscus are self-organizing by the interaction of the plasma and beam particles.[8] In a ray-tracing code, however, a model is needed to determine the nature of the plasma/beam boundary. In comparing PBgun and SEFI to experiment, we are in large part gauging the validity of these various schemes in simulating the plasma/beam interface.

There are many marks by which such codes can be judged but two simple and effective experimental methods are extracted current and the angular divergence of the beam envelope. A more extensive parameter for beam diagnosis is emittance but since our experimental equipment was not equipped with a pepper pot or other instrument for measuring beam emittance no direct comparison of this quantity is presented in this article. Tinschert and Zhao have, however, already published a comparitive study of emittance between AXCEL-GSI and the CHORDIS ion source which showed quite good agreement between simulation and experiment. Unfortunately, they only did so for a limited range of extraction parameters.[9] Wituschek again presented a comparitive report on emittance based on the same systems, but offered no interpretive discussion of the results.[10] Both articles found

[a]Author to whom correspondence should be addressed; electronic mail: orson.sutherland@anu.edu.au

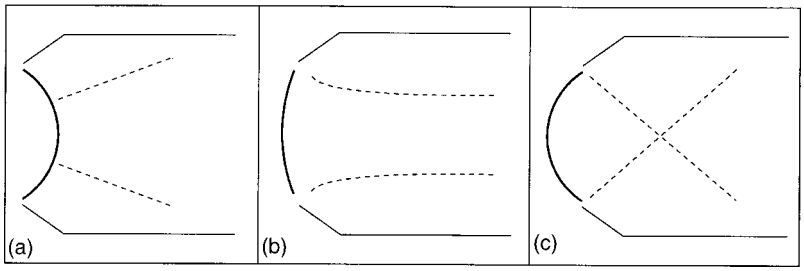

FIG. 1. Diagram showing the evolution of the beam shape as a function of extraction voltage. (a) Convex meniscus: the beam is divergent. (b) "Cross-over meniscus:" the beam is parallel. (c) Concave meniscus: the beam is convergent.

good correlation between simulation and experiment for extracted current. Though it is conceded that emittance is an important quantity, experimentally extracted current and beam divergence are more easily measured. In this article we are interested in determining whether or not the models implemeted in the simulation codes can predict the correct physics in the plasma/sheath region and thus get the extracted current correct and the resulting angular divergence of the ion beam. Of particular interest is extraction of bright ion beams from a plasma source. It should be noted, however, that if a strong correlation or understanding is shown for the extracted current or divergence, it does not translate to accuracy in predicting brightness. This is because these codes have round off error, or numerical diffusion,[11] which increases the emittance and decreases the brightness that is calculated. This effect will not be covered in this article.

II. EXTRACTION FROM A PLASMA

The extraction of ions from a plasma is governed by an equilibrium between the ambipolar flux of ions to the extraction aperture and space charge effects in the extractor. Ambipolar flux is taken to be

$$J^+ = 0.6 \cdot e \cdot n \cdot C_s , \tag{1}$$

where e is the elementary charge, n is the bulk plasma density, and C_s is the ion sound speed.

It is generally assumed that the space charge effects in the extractor are governed by Child's law[12]

$$j^+ = K \cdot \left(\frac{e}{M} \right)^{1/2} \cdot \frac{V_{\text{ext}}^{3/2}}{X^2} , \tag{2}$$

where j^+ is the current density in the extractor, K is an arbitrary constant related to the system geometry, M is the atomic mass of the working gas, V_{ext} is the applied extraction voltage, and X is the distance over which V_{ext} is applied. Equation (2) requires, holding all other things constant, that the current density in the extractor increases with increasing applied voltage. But, according to Eq. (1) this can clearly not happen if the plasma density and electrode geometries are unchanged. Thus K must evolve to meet the equilibrium requirements of the extractor, where K is related to the shape of the plasma/beam interface, or meniscus. This is justified experimentally in the literature by observing the evolution of beam form as a function of extraction voltage or extracted current.[12]

As the extraction orifice is circular in our experiment, the flow of particles in the extractor can be thought of as a cone of current flowing between two concentric spheres. A solution to the Child law under the assumption of current flow between concentric spheres was given by Langmuir and Blodgett.[13]

III. EXPERIMENTAL METHOD

A. Extracted current

A basic condition for the existence of a plasma is the conservation of particle flux. This requires that an equal number of electrons and ions are lost to the plasma boundary. To compensate the loss of ions through the extraction aperture, electrons are removed by the extraction voltage bias electrode in equal number. This current can be measured and is equal to the extracted beam current.

B. Angular divergence

The changing shape of the plasma meniscus leads to three different beam forms.[12] Assuming zero ion temperature, a sufficiently concave meniscus results in a convergent beam and a sufficiently convex meniscus produces a divergent beam. At some point between being convergent and divergent, the plasma meniscus is such that the extracted beam is parallel (Fig. 1). Though experimentally ion temperature is not zero and space charge, especially in the acceleration gap of the extractor, cannot be ignored, the concept of a singular transition point between convergent and divergent beam forms leads to a simple experimental method for determining when a beam is parallel or slightly divergent in the transport region. However, it must be noted that if the ion beam past the third electrode is not completely space charge neutral and of low emittance it will be parallel only over a short distance so that a slightly divergent beam, having a larger waist, may have less divergence further downstream than the beam that was first parallel after the extractor.

The Decel electrode in our experiment (Fig. 2) is 52 mm in length and 19 mm in inner diameter which represents a solid half angle of 10° from the extractor orifice to the exit of the electrode system. If an extracted beam has a divergence angle greater than this, some portion of the beam will strike the electrode resulting in a measurable current I_3. This current will increase as the beam becomes more convergent or divergent. As a result, a minimum in the Decel current is observed when sweeping the extraction voltage from a strongly divergent to a strongly convergent regime, while keeping the plasma density constant. This is the point where we consider the beam to be parallel or slightly divergent.

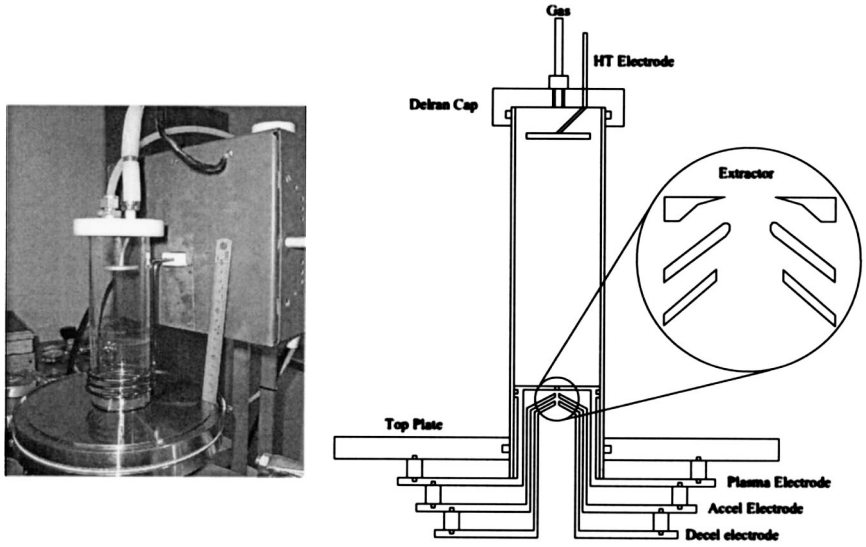

FIG. 2. Left: a photograph of the system. Right: a diagram of the system.

IV. EXPERIMENTAL SETUP

A. Vacuum system

The experiment consisted of an inductively coupled plasma source, an extraction assembly, and a vacuum tank. The extraction assembly slid into one end of the plasma source and clamped down onto the top of the vacuum chamber, connecting all three components together (Fig. 2). A Delrin cap terminated the top of the plasma source which was a 5-cm-diam, 25-cm-long Pyrex tube. The vacuum tank was a 20-cm-diam, 30-cm-long stainless steel cylinder with a side mounted flange to accommodate a 100 l/s turbomolecular pump. Base pressure was maintained at 10^{-6} Torr.

The extraction orifice was 1.5 mm in diameter and due to the low conductance that this and the rest of the extractor represented, a significant pressure gradient existed between the source and the vacuum tank when a feed gas was introduced to the source. Lack of space on the Delrin cap meant that a seperate pressure gauge for the source was impractical. Instead an ion gauge mounted on the vacuum tank was used to infer pressure in the source. An initial test was conducted where the source pressure was monitored as a function of the pressure inside the vacuum tank using a Convectron gauge mounted on a specially made source cap. There was a very clear linear relationship between the two pressures with a ratio of almost exactly 100 to 1 between the source and the vacuum chamber which agreed very well with the values of conductance calculated from the theory.

B. Gas and rf

The working gas was Krypton and was introduced via a needle valve through the Delrin cap situated at the top of the glass tube. The mass flow rate was not measured directly. The rf system consisted of a three-turn loop antenna situated near the extraction end of the source tube and was driven via a Π matching network at a frequency of 13.56 MHz (Fig. 2). Reflected power was monitored using a standing wave ratio and power meter and was less than 5% of forward power for any given experiment. No attempt was made to measure the temperal variation of either the plasma or floating potentials. It is noted, however, that the proportion of capacitive coupling in such plasmas is relatively small. Input power was restricted to less than 200 W to avoid excessive heating of the antenna and glass tube. Cold air was blown over the apparatus to maintain a tolerable working temperature.

C. Plasma source

Measurements of the source plasma density were taken using a dog-legged cylindrical Langmuir probe,[14] 50 μm in diameter and 5 mm long. The probe was introduced through the Delrin cap using an axially translating ceramic tube 2 mm in diameter. The probe tip could not be placed closer than 2 mm to the plasma electrode because of arcing. For simplicity, density at the extraction orifice was assumed to be the same as that at 2 mm above the extractor.

Despite the low input power, relatively high densities where achieved. Figure 3 shows density versus pressure for various input powers at 2 mm above the bottom of the plasma source. At 5 mTorr and 200 W, the density was $1.5 \times 10^{12}\,\mathrm{cm}^{-3}$. As pressure was increased density fell and though not measured it was expected that density would also

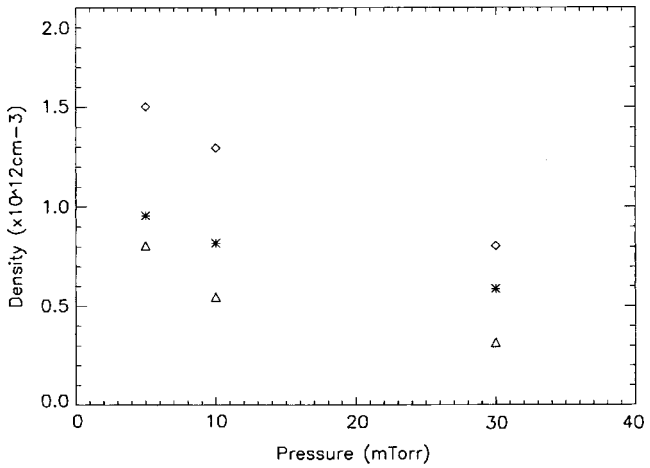

FIG. 3. Plot of density vs pressure for various input power levels at 2 mm above extraction orifice. △: 50 W, ∗: 100 W, and ◇: 200 W. Measurements were not taken below 5 mTorr but it is expected that the density falls off.

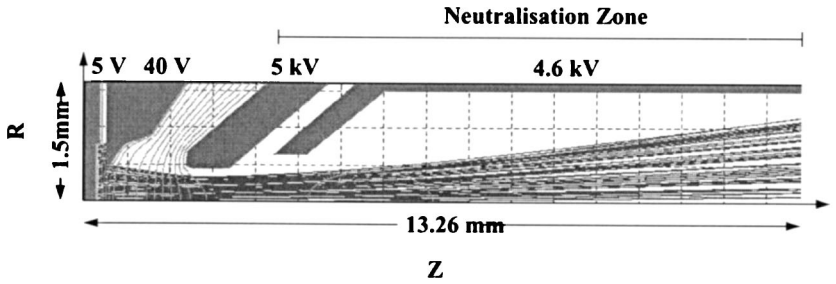

FIG. 4. Graphical output from a PBgun simulation overlayed with axes for a cylindrical coordinate system. R represents the radius from the center and Z the distance along the axis of symmetry. Extraction voltage is 4.6 kV. Here, the Accel and Decel electrodes are charged relative to the substantially grounded plasma electrode as the ions are negatively charged in PBGun (their mass is still that of Ar). The plasma electrode is 35 V above the emission surface to simulate the plasma sheath. The program chooses every *n*th trajectory for graphical display where *n* is not necessarily a multiple of the number of points taken from the Maxwellian at each starting position, hence an apparent nonhomogeneity. This, however, is not reflected in the actual beam current density distributions. The "neutralization zone" is the region over which some percentage of beam neutralization is applied. In this simulation 2% neutralization was employed. Courtesy of John Keller.

have fallen off for pressures below 5 mTorr. This trend as a function of pressure was valid for all three powers used and it was found that for any given pressure, increased power resulted in augmented density.

D. Extraction system

The experiment was equipped with an axially symmetric single orifice three-electrode extraction system, shown in Fig. 2. It consisted of a floating Plasma electrode which charged to V_1, approximately $5kT_e$ below the plasma potential (of between 0 and 8 kV), an Accel electrode with an applied voltage V_2 of -400 V, and a Decel electrode which was grounded. The plasma was charged up to the extraction voltage by a bias electrode introduced through the Delrin cap and the plasma electrode voltage verified with a voltmeter via a vacuum feedthrough.

E. Beam neutralization

Though not obviously *a priori* in the Australian National University system, the beam was partially self-neutralizing by the presence of a beam plasma which presumably provided sufficient negative charge to neutralize a nonnegligeable beam space charge. The level of neutralization was not measured, neither was the exact creation mechanism for this beam plasma investigated, either experimentally or in simulation. A simple photograph of the beam taken through a window installed on the vacuum tank 10 cm below the extraction system alerted us to its presence (Fig. 6). That there was a faint violet light was an indication that some excitation mechanism was in progress. It was not clear, however, if the light emission was from the beam ions or the slow plasma ions. Two mechanisms for the formation of this beam plasma are ionization and secondary electron emission from sputtering of surfaces in the diagnostic chamber. In our system ionizing collisions can be ignored in the extraction and transport regions on account of the low pressure there (10^{-5} Torr in the diagnostic chamber and some distribution from 10^{-3} to 10^{-5} Torr in the extractor) and low beam energy (less than 6.1 kV). Spädtke presented modeling showing the degree of neutralization reached in the system and proposed that this was due to surface sputtering.[6] Indeed, the pressure in that experiment was also sufficiently low as to preclude ionizing collisions. However, again in that case the precise mechanism was not observed in simulation or experiment.

V. SIMULATION STRATEGY

The simulation strategies employed in this work will only be described briefly here. For an excellent overview of ion beam extraction codes the reader is referred to Spädtke.[6]

A. Ray tracing

Ray-tracing codes employ the Lorentz force law to calculate the trajectories of particles emanating from an emitting surface (Fig. 4). Superficially, the problem is that of how to determine the electric field for use in this relation. The magnetic field is ignored since the beam particles are well below relativistic velocities and no external magnetic field is applied. The electric field potentials produced by the extraction electrodes are calculated using a numerical approximation to Laplace's equation. Space charge fields are determined from the beam charge density distribution. The field due to each trajectory is calculated using Poisson's equation and superposed to determine a space charge potential distribution for the extractor as a whole. This suggests an iterative approach to determining beam trajectories. First, the field is determined from the electrode geometries and space charge fields, then the individual trajectories are calculated using the Lorentz force law. Once all the trajectories have been determined in this way, the space charge fields are recalculated and the process repeated until the simulation converges.[4] Collisions with neutrals are not incorporated into the simulation.

The question arises with simulations of this type as to how best to model the plasma meniscus.[4,5] PBgun uses a fine mesh region near the plasma meniscus which greatly increases the accuracy and stability of the code. This region is called the emission surface and its location is specified by the user. It starts with a defined surface in the plasma presheath from which the defined ion current or current density is initiated. Then by determining the space charge due to both the ion beamlets and the electrode density, the potentials are solved using Poisson/Laplace iterations. These ion beamlets are assumed to start out with a Maxwellian distribution due to the defined ion temperature. Thus the fine matrix equi-

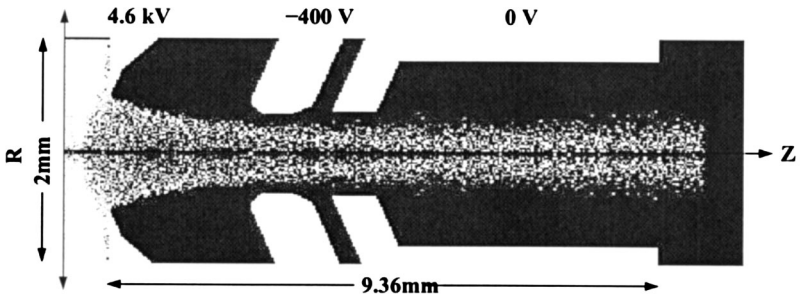

FIG. 5. Graphical output from a SEFI simulation overlayed with axes for a cylindrical coordinate system. As with the PBGun simulation, extraction voltage is 4.6 kV. Here the Ar ions have their customary positive charge and hence the electrodes are charged as expected. The sheath voltage does not need to be specified in the electrode potentials as the hybrid PIC develops sheath potentials automatically. The plasma source has been shortened to simplify graphical display but the meniscus is still clearly discernible. A hollow in the beam and plasma is evident and is an artifact of the "R=0" problem for such simulations. Courtesy of Michael Irzyk.

potential lines, one of which is the meniscus equipotential line, are determined. The meniscus equipotential cannot touch the starting surface and the user specifies an electron temperature, ion temperature, and ion current over a given area (hence an ion density) and initial ion energy. The electron space charge density is handled by using Poisson's equation. The ion space charge density is determined from the ion trajectories and the voltage on the grid points with the beams starting perpendicularly to the initial emission surface with a Maxwellian distribution of angles, corresponding to the ion temperature. Here, we try to make the defined starting surface close to that of the Bohm sheath boundary as this increases the stability and reduces the number of iterations needed for a given accuracy. These calculations were carried out to a minimum of 50 iterations with a "convergence requirement for voltage relation" of $2e^{-7}$. The nonuniformity of ion rays in Fig. 4 is an artifact of the plotting tool, which only displays a small percentage of the total number beams. It was noted, however, that the ion current density was uniform two grid points or more from the axis.

B. Boltzman particle-in-cell (PIC)

SEFI is similar in concept to PBgun in that it employs the Lorentz force law to determine particle trajectories from the local field conditions but differs in its treatment of the plasma and the extracted particles (Fig. 5). SEFI is a hybrid particle-in-cell code, where ions are treated individually rather than by the trajectory that they infer. As this article deals with techniques rather than the specifics of code, a full description of hybrid PIC and SEFI in particular is given elsewhere.[15,16] Briefly, PIC is a time dependent simulation method where particle and field "states" are calculated at regular intervals (usually on the order of the picosecond). At every time step the field is calculated using Poisson's law based on the position of each particle. All particles are then accelerated according to the Lorentz force law. Because, in the simplest case, the code has to account for every particle in the simulation, it is computationally expensive. One way to decrease the convergence time to steady state is to assume a collisionless plasma in which electrons are distributed according to the Boltzman relation. Because in this case electrons would no longer need to be treated individually, a time step on the order of one tenth of a plasma oscillation would no longer be required and could instead be set to some fraction of the ion transit time between adjacent mesh elements. This yields at least a three order of magnitude improvement in computation time.

VI. RESULTS

Figures 7 and 8 show experimental data overlayed with data from PBgun and SEFI. In Fig. 7 there are two sets of experimental data collected on separate occasions using the same experimental conditions. Only the data from the second experiment appears in Fig. 8 because no angular divergence measurements were taken for experiment 1. In both experiments pressure was set to 10 mTorr and input power to the matching network was maintained at 200 W. No magnetic field was employed. Reflected power was less than 5%.

A. Extracted current

All the curves show a monotonically increasing relationship between extracted current and extraction voltage. The

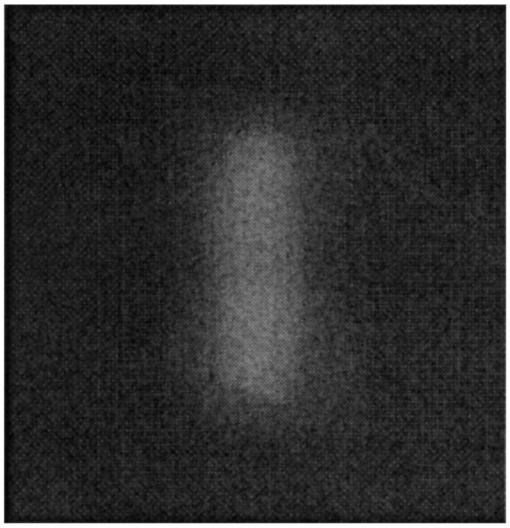

FIG. 6. Image of the beam plasma. Photo taken through 25-mm-diam circular window in the side of the diagnostic chamber, 100 mm below extractor.

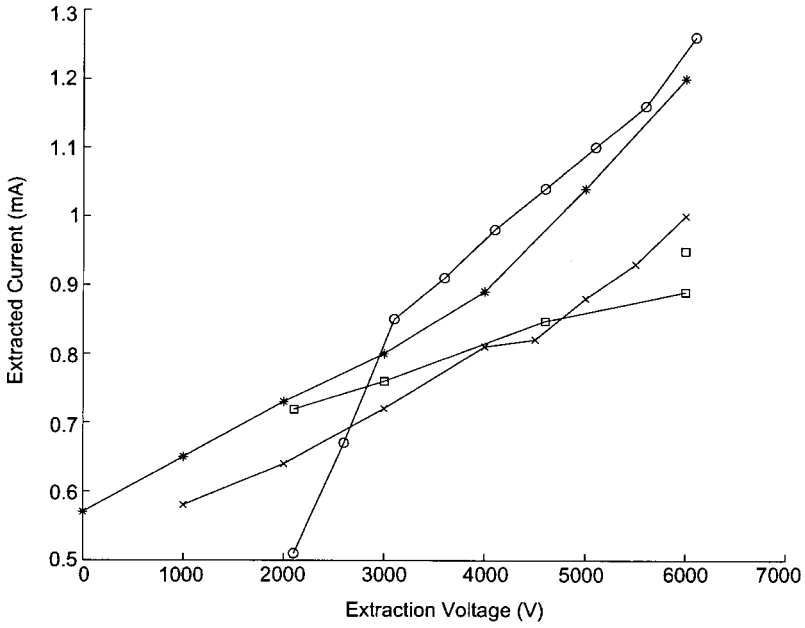

FIG. 7. Extracted current vs extraction voltage. ⋆: Experiment 1, ×: Experiment 2, ○: SEFI, □: PBgun. Note: two points are calculated in PBgun at 6 kV. The lower of the two corresponds to the initial emission surface being placed at the plasma edge (as for all previous points). The higher point corresponds to the initial emission surface being placed deeper into the plasma at 0.15 mm from the edge.

experimental curves have a slight bow to them which may be indicative of a power law. On the other hand, most of this curvature may be due to secondary electrons returning to the source from ions striking the Accel electrode. For the same ratio of $J^+/V_{\text{ext}}^{3/2}$, or the same value of "K" in Eq. (2), the experiment 2 data has a plasma density of roughly 0.77 of the experiment 1 data.

It is noted that extracted ion current is not nil for zero extraction voltage. This is expected because, in the presence of a plasma, ions and electrons still flow to the extraction aperture but only ions escape since electrons remain blocked by the presence of the Accel voltage.

The extracted current plotted for the SEFI data is the extracted current minus the ion current to the Accel electrode, which is essentially zero above 3 kV. SEFI matches the experimental results of experiment 1 quite closely above 3 kV but deviates very strongly from the experimental data below this, where the Accel current becomes non-negligible, increasingly underestimating extraction current as the amount of current striking the Accel increases. In the SEFI data a plasma density of $10^{12}\,\text{cm}^{-3}$ was used from the density measurements in Fig. 3. With this density the SEFI data match very closely the results of experiment 1, both in magnitude and function where the Accel current is essentially zero. If a density of $0.9\times10^{12}\,\text{cm}^{-3}$ were used the SEFI data would overlay the experiment 1 data within a reasonable experimental error above 3 kV. Thus as expected the SEFI code handles the plasma and the plasma sheath properly. It is noted that, except for the last point, the SEFI data are quite linear in this range.

In the PBgun data, a current density was used which matched the extracted current near 4.6 kV of the experiment 2 data. For most points this current density was specified near the position of the plasma meniscus which was deter-

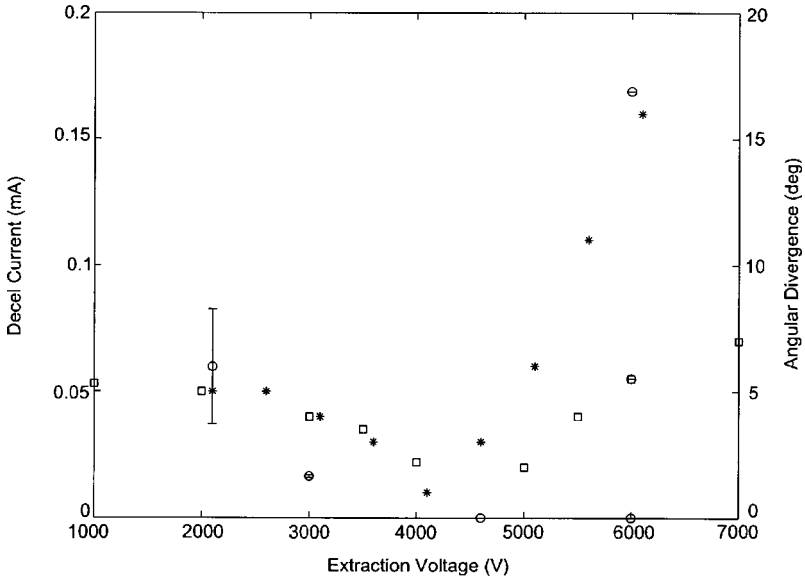

FIG. 8. Decel electrode current (left axis) and angular divergence (right axis) vs extraction voltage. Note: there is no functional relationship between left and right axis. □: Experiment 2, ○: PBgun, ∗: SEFI. Error bars on PBgun data represent the range over which the solution oscillated between successive iterations; in this case there is no steady state solution. At 6 kV there are three PBgun points representing from top to bottom, 0%, 25%, and 90% neutralization.

mined self-consistently by the code. This plasma boundary is determined by the propagation of rays emanating from the initial emission surface with a defined current and Poisson's equation for the electrodes. Thus this surface acts as the plasma bulk. The result of this is a linear curve with a slope of roughly 60% of that of the experiment 2 data set. To see the effect of specifying the current deeper in the plasma a second point was calculated at 6.0 kV. This gives almost the same extracted current as that measured in the experiment 2 data set at 6.0 kV. Thus it can be concluded that for a thin plasma aperture roughly 40% of the current variation due to the extraction voltage occurs in the plasma pre-sheath and roughly 60% occurs in the sheath. That is, there is an apparent expansion or compression of the plasma ion drift current in the pre-sheath, which changes the value of the ion current density near the meniscus of the sheath boundary. This expansion or compression is a function of the extraction voltage. The change in the shape of the meniscus also changes the shape of the ion beams in the sheath, which changes the extracted current for a given current density at the plasma meniscus. PBgun and similar codes can calculate the latter but are very unstable when trying to calculate the former. It is most probable that for a thick plasma aperture the plasma pre-sheath effect would represent a much larger proportion of the overall variation in extracted current as a function of extraction voltage.

B. Angular divergence

Figure 8 shows the data for the Decel electrode current measured experimentally and in the PBgun simulation. Overlayed on this are the angular divergence measurements for SEFI. Though electrode currents can quite easily be measured in SEFI, the Decel electrode in the simulation was made too short and so the collected currents could not be directly compared with the experimental or PBgun results. Instead, the angular divergence of the beam envelope was measured as a function of extraction voltage using output graphs such as Fig. 5. A direct comparison between electrode current and angular divergence is not possible, but the general form of the curve and the location of the associated minimum should be the same. Indeed, all three curves share the same form and a clear minimum between 4 and 5 kV can be discerned in each case. In particular, the PBgun calculation for 4.6 kV gives a slightly divergent beam with no Decel current. This appears to be consistent with the experiment 2 data set and other experimental data taken at different power densities. For the SEFI simulation, the minimum appears to occur at 4.3 kV.

To gain some idea of the neutralization in the extracted beam three points were calculated in PBgun at 6 kV. This extraction voltage was chosen since the beam waist is smallest there and hence its divergence most sensitive to the amount of beam neutralization. For 90% neutralization, none of the beam impinged on the Decel electrode resulting in a zero current. For 25% neutralization, a similar current was obtained to that measured in experiment 2. And finally, with no neutralization divergence was, as expected, at its strongest. Though the exact amount of experimental neutralization is not known, especially since the amount of beam steering from possible misalignment at the Accel electrode was unclear, the estimate of the neutralization from the calculation at 6 kV would seem to be at least 25%. Therefore, a neutralization of 25% was used for the remaining points calculated in PBgun, though it is noted that these points were not very sensitive to the level of neutralization. The SEFI data were calculated with no neutralization.

The PBgun calculations at 3.0 and 2.1 kV both resulted in current striking the Accel electrode. This caused some error or oscillation in that portion of the beam which missed the Accel electrode and struck the Decel electrode. The range shown is for six consecutive iterations after at least 30 total iterations. Since, in general, it is not desirable to operate the extractor with such large Accel current it does not seem to be a significant shortcoming of the code.

C. Discussion of extracted current and angular divergence simulations

PB gun and SEFI both appear to have problems simulating beams which cross over the axis. This is not uncommon with particle beam simulation codes. The authors' experience of IGUN is that it also has trouble calculating near axis beam trajectories. In PBgun v4.0, when a Maxwellian distribution is used for the emitted ions to simulate ion temperature, there is a peak in beam density and thus space charge on axis which causes the meniscus to move too much toward the Accel electrode and thus increase the convex curvature of the meniscus.

The opposite, and possibly larger effect, is seen in the SEFI code. Here the current on axis is depleted (Fig. 5) which causes the meniscus to move into the plasma near the axis and increases the concave curvature of the meniscus. This in turn may be why the SEFI data in Fig. 8 go through a minimum in divergence at a lower extraction voltage than either the experimental data or the PBgun simulations. It is also probably why extracted current for a given plasma density was larger relative to the experiment 2 data, since the greater the curvature, the larger the extracted current.

If one is interested in starting from a given plasma density, then it appears from this work that a PIC simulation for the plasma is quite beneficial. On the other hand, if the current density is specified near the meniscus then ray-tracing codes, such as PBgun, are most adequate. For a thick electrode, which may have a complex meniscus shape, a PIC code may be the best option.

[1] E. W. MacDaniel, *Collision Phenomena in Ionized Gases* (Wiley, New York, 1964).
[2] R. L. Seliger, R. L. Kubena, R. D. Olney, J. W. Ward, and V. Wang, J. Vac. Sci. Technol. **16**, 1610 (1979).
[3] J. Cleaver and H. Ahmed, J. Vac. Sci. Technol. **19**, 1145 (1981).
[4] J. E. Boers, *PBguns, An Interactive IBM PC Computer Program for the Simulation of Electron and Ion Beams and Guns*, Thunderbird Simulations, v4.01 edn. (1999).
[5] R. Becker and W. B. Herrmannsfeldt, Rev. Sci. Instrum. **63**, 2756 (1992).
[6] P. Spädtke, Rev. Sci. Instrum. **63**, 2647 (1991).

[7] P. Spädtke and C. Mühle, Rev. Sci. Instrum. **71**, 820 (2000).
[8] C. K. Birdsall and A. B. Langdon, *Plasma Physics via Computer Simulation* (McGraw–Hill, New York, 1985).
[9] K. Tinschert and W. Zhao, Rev. Sci. Instrum. **63**, 2782 (1991).
[10] H. Wituschek, Rev. Sci. Instrum. **63**, 2785 (1991).
[11] P. Roache, *Fundamentals of Computational Fluid Dynamics* (Hermosa, 1998).
[12] W. L. Rautenbach, Nucl. Instrum. Methods **12**, 169 (1961).
[13] I. Langmuir and K. B. Blodgett, Phys. Rev. Lett. **22**, 123 (1923).
[14] M. A. Lieberman and A. J. Lichtenberg, *Principles of Plasma Discharges and Materials Processing* (Wiley, New York, 1994).
[15] M. Irzyk, Ph.D. thesis, Université d'Orléans, 2001.
[16] K. L. Cartwright, J. P. Verboncoeur, and C. K. Birdsall, Phys. Plasmas **7**, 3252 (2000).